Mussels blow rings: Jet behavior affects local mixing

Michael Nishizaki[a] Josef Daniel Ackerman*

[1]Physical Ecology Laboratory, Department of Integrative Biology, University of Guelph, Guelph, Ontario, Canada

Abstract

Benthic suspension feeders such as dreissenid mussels (*Dreissena polymorpha* and *D. rostriformis bugensis*) are often found in remarkably dense aggregations (i.e. $> 10^5$ mussels m^{-2}), which is surprising, given their high clearance rates and limited mixing within the benthic boundary layer. Results from flow visualization in flow chamber experiments indicate that there is indeed limited mixing around mussel aggregations at low flows and that siphonal jets can increase mixing around and above these aggregations. Using particle image velocimetry (PIV) to further investigate the underlying hydrodynamics of these jets, we characterized differences in velocity and vorticity among four siphonal behaviors (e.g., slow flux, streaming, exhalant jets, and inhalant jets), including both continuous and pulsatile jets, the latter of which generate free vortex rings. Incorporating these hydrodynamic characteristics into a computational fluid dynamic (CFD) model revealed that siphonal jets increased mixing, expressed as vertical diffusivity in the benthic boundary layer. These differences were most pronounced at slow vs. fast cross-stream velocities, but those differences diminished several body lengths (i.e. 10^{-1} m to 10^{-2} m) downstream. The results from PIV measurements and CFD modeling suggest that benthic suspension feeders can influence patterns of local mixing, which would affect mass transport and biogeochemical processes in the near-bed region. This underscores the need for physical-biologically linked models to incorporate the behavior of benthic suspension feeding invertebrates.

In aquatic ecosystems, many benthic organisms feed by removing suspended material from the water column (e.g., Wildish and Kristmanson, 1997). These suspension feeders are often numerically dominant species that impart a wide range of ecological impacts on phytoplankton, benthic algae, other invertebrates and fish (Conroy et al., 2005; Vanderploeg et al., 2010; Higgins et al., 2014; Sebens et al., in press; see reviews in Gilli and Coma, 1998; Ackerman, 2014). By removing suspended material from the water column, suspension feeders also play important roles in regulating water clarity, dissolved oxygen concentrations, and nutrient cycling (North et al., 2012; Cha et al., 2013; Greene et al., 2015; see references in Nalepa and Schloesser, 2014). Although they represent an important link between benthic and pelagic habitats (Ackerman et al., 2001; Hecky et al., 2004), the activity of many bottom dwellers may be limited by low mixing rates in the benthic boundary layer (BBL) (Frechette et al., 1989; Ackerman et al., 2001; Reidenbach et al., 2013). The exhalant jets from active feeders contain momentum (O'Riordan et al., 1995), and some work indicates that these types of jets increase mixing of near-bottom waters (O'Riordan et al., 1995; Larsen and Riisgård, 1997; Lassen et al., 2006; van Duren et al., 2006), whereas others suggest that they do not (Smaal et al., 1986; Ertman and Jumars, 1988). The degree to which these biogenic flows enhance mixing in the BBL is an important question given the limited exchange of food, dissolved gases, and waste products between benthic organisms and the water column, especially at high organism density and lows flows.

Dreissenid mussels [zebra mussels, *Dreissena polymorpha* (Pallas) and quagga mussels, *Dreissena rostriformis bugensis* (*Andrusov 1897*)] have invaded many aquatic habitats, achieving extreme population densities (e.g., $> 10^5$ mussels m^{-2}; Schloesser and Kovalak, 1991). The gregarious nature of dreissenid mussels potentially leads to local food/seston depletion (Jørgensen, 1990; Ackerman et al., 2001; Smith et al., 2007), potentially limiting feeding (Schneider et al., 1998; Boegman et al., 2008) and metabolic activity (Stoeckmann and Garton, 1997; Tyner et al., 2015). Given that limited near-bed mixing is likely to have important ecological and physiological consequences, it is reasonable to investigate the potential for siphonal feeding behavior to increase local mixing. This question is particularly relevant given that dreissenids display wide variation in clearance rates (Kryger and Riisgård, 1988; Bunt et al., 1993; Ackerman, 1999), and

*Correspondence: ackerman@uoguelph.ca

[a]Present address: The James T. Carlton Marine Science Center and The Maritime Studies Program, Williams College and Mystic Seaport. Mystic, CT, USA.

there is evidence that other suspension feeders use multiple modes of feeding behavior (Riisgård and Larsen, 2010; Nishizaki and Carrington, 2014).

The purpose of this study is to examine the fluid dynamic properties of siphonal jets of dreissenid mussels to determine how biogenic jets affect mixing in the BBL using a combination of experimental and theoretical techniques. We begin by assessing flow patterns in the BBL surrounding both individuals and aggregations of mussels using dye/labeled algae releases and continue with detailed measurements of the hydrodynamic properties of siphonal jets using particle imaging velocimetry (PIV). With these data, we use computational fluid dynamic (CFD) models to determine the effect that different mussel siphonal jet behavior has on local mixing under different cross-stream water velocities.

Materials and methods

Flow visualization of exhalant jets

Limestone rock samples colonized by zebra and quagga mussels were collected at a depth of 0.75 m from Lake Erie (42.79°824′N 80.06°623′W). Mussels on the bottom and sides of the rock had a shell length (SL) of 1–2 cm, whereas those on the top also included SL of 1–3 cm at a density of ~2.3 × 10^4 mussels m^{-2}. Mussels were maintained at 15°C in aerated aquaria using 0.2 μm filtered lake water and fed live algae (equal portions of *Selenastrum* [UTCC-37], *Scenedesmus* [UTCC-10], and *Chlorella pyrenoidosa* [UTCC-90]; University of Toronto Culture Collection). Samples were allowed to acclimate to test conditions (19°C) for several days before experiments.

Larger-scale visualizations around a rock colonized with dreissenid mussels was conducted in a large flow chamber (0.38-m wide × 0.31-m high × 10-m long) filled with tap water several weeks prior to the experiments allowing sufficient time for off-gassing of chlorine. At the beginning of the experiment, the limestone rock was placed in mid channel at a downstream distance of 4.27 m. Experiments were conducted at 19°C under no flow and at a velocity, $U \sim 4.4$ cm s^{-1}, estimated from the timed dispersion of dye. Near bed velocities of < 10 cm s^{-1} have been reported from zebra mussel beds in the field (Ackerman et al., 2001). Reynolds number (ratio of inertial to viscous forces; $Re = lU/v$, l = length and v = kinematic viscosity) based on the hydraulic diameter of the channel was 2073 and 5940 for the (length) rock. Under the no-flow conditions, dye labeled *Chlorella* culture was released in a continuous stream in the vertical direction by slowly pulling the injector away from the bottom. Conversely, it was released as discrete blobs at ~2 cm height increments above the rock under flowing conditions to visualize flow over the rock. Images were recorded using a SLR camera and using a CCD camera fitted with a 100 mm-macro SLR lens. Video sequences were digitized using a PCVISIONplus Frame Grabber (Imaging Technology) at two images per second at a resolution of 640 × 480 pixels with 256 gray levels.

Flow visualizations around individual or small aggregations of zebra mussels were conducted in a small recirculating flow chamber (0.17-m wide × 0.10-m high × 1.7-m long; Ackerman and Nishizaki, 2004) using fluorescein-labeled *C. pyrenoidosa*. Chamber water depth was 8.5 cm using 0.2 μm filtered lake water (15–18.5°C) and operated at $U \sim 3.5$ cm s^{-1} as indicated from the timed movement of dye. Mussels were placed in mid channel 56 cm downstream from the last collimator (flow straightener). The *Re* of the channel was 454 and *Re* based on individual mussel length was 200–400. Dye and/or labeled algae were released at various heights around the mussels and near their inhalant siphons.

Characterizing mussel jets using particle image velocimetry

Zebra mussels were collected from Lake Ontario (43.30°185′N 79.80°177′W; 1-m depth) and maintained in aerated aquaria containing filtered lake water in the Hagen Aqualab at the University of Guelph. Mussels were fed dried *Chlorella* (Prime Chlorella, Calgary, AB). Flow fields surrounding mussels were quantified using 2D PIV as described by Nishizaki and Ackerman (2005). Briefly, the PIV system incorporates a pulsed laser (Lasiris Magnum SP diode laser, StockerYale; Model 500 Pulse Generator, Berkeley Nucleonics) with a high resolution progressive scan camera (TM-9701, PULNiX America) and an image acquisition system operating at 30 Hz (Road Runner Hardware, BitFlow Inc; Video Savant Software Ver. 3.0, IO Industries). The camera was fitted with a dissecting microscope binocular (Nikon, SMZ-2T) that allowed for side-viewing of the tank. Pairs of images, each of which was recorded per laser pulse, were used to analyze water motion (e.g., velocity and vorticity) with PIVView 2.1 software (PivTec GmbH).

Individual zebra mussels (SL = 2.75 ± 0.27 cm [mean ± SE]) were placed in a 20 L aquarium (51 × 28 × 33 cm) under no flow conditions near the center of the tank to avoid wall effects. Mussels were acclimated for 5 min in 17°C water seeded with *Ankistrodesmus* sp. obtained locally. Water was changed between each trial and mussels were used only once in experiment. The hydrodynamic jet structure was defined as the area where velocities were greater than twice the maximum background flow speed. Siphonal jet velocities and vorticities were measured from within this area over the duration of each trial.

Differences in velocity and vorticity among the different behaviors were assessed with ANCOVA, with mussel shell length as a covariate. All analyses were conducted using SPSS v22.0 (IBM Corp., New York, NY).
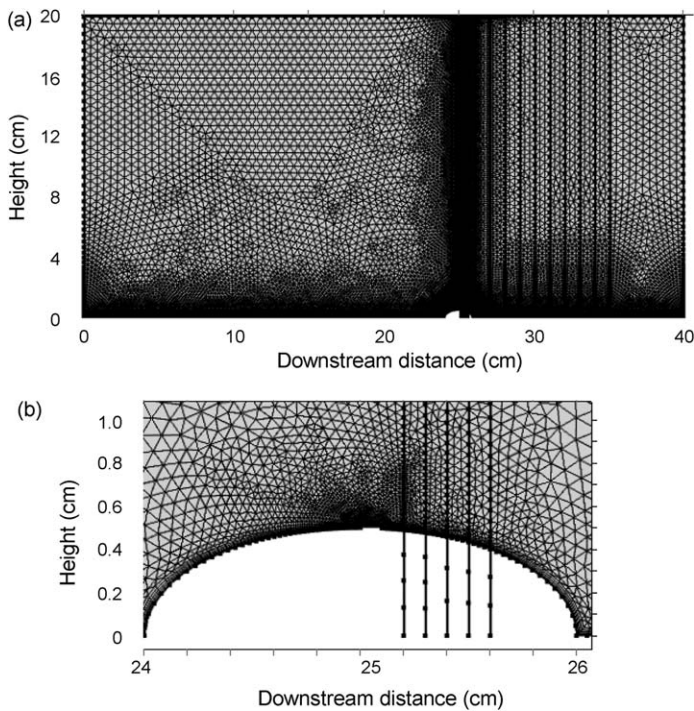
Fig. 1. The computational geometry used to model the hydrodynamics of scalar distribution around a dreissenid mussel. Vertical lines represent sampling transects (e.g., for scalar concentration) that did not interfere with velocity or scalar concentration fields. Panel (**a**) depicts the entire spatial domain and panel (**b**) highlights the region surrounding the mussel.

CFD modeling of the effects of exhalant jets on local mixing

We investigated the effect of mussel exhalant jets on local mixing using CFD modeling via a 2D finite element model of flow and scalar transport around a single dreissenid mussel (COMSOL Multiphysics v4.4, Burlington, MA). Water motion was modeled within a rectangular domain (length = 40 cm, height = 20 cm) around a mussel (length = 2 cm, height = 1 cm) placed 25 cm downstream from the leading edge (Fig. 1a). The 0.1 cm wide siphon was located flush with the top of the mussel (Fig. 1b). A 2D k–ε model, a type of Reynolds-averaged Navier-Stokes model based on Reynolds decomposition (i.e. time average vs. fluctuations) was used to simulate flow (Davidson, 2004). Water entered the domain from the left vertical boundary and exited through the right vertical boundary. The upper boundary was open with limited viscous stress (e.g., normal stress = 0 N m^{-2}), whereas the lower boundary was defined by the no-slip condition. The spatial domain was modeled using a free mesh containing 24,144 triangular elements (Fig. 1), which was compared to high resolution simulations containing 129,534 triangular elements. Preliminary simulations run under normal and high resolution grid size produced quantitatively and qualitatively similar results, especially within 5–6 mm downstream of the mussel,

demonstrating grid independence in the model (i.e. grid convergence). Water was also introduced from the siphon using the mean velocity and vorticity measured for each behavior using PIV (see Results). For pulsatile behaviors, jets were controlled with a Gaussian pulse function that limited the duration of the pulse (2 s, based on observations from flume and PIV). To determine vertical diffusivity (D) generated from physical mixing alone (i.e. no behavior control), simulations were run with no exhalant jet (e.g., no velocity or vorticity introduced from exhalant siphon). Simulations were run for 600–1300 s to provide sufficient time for flow development in the model domain.

A 2D convection-diffusion (i.e. mass balance) model was paired with the hydrodynamic model to simulate the interaction between fluid motion and solute concentration. Scalar concentration at the beginning of the simulation was set at 0.001 mol m^{-3} throughout the spatial domain with input of 0.001 mol m^{-3} from the left vertical boundary. Scalar was also introduced from the horizontal face of the siphon at 1 mol m^{-3} and the diffusion coefficient of the scalar in water was set to 10^{-9} m^2 s^{-1}, which is typical for many solutes in freshwater (Canfield and Green, 1985; Saltzman et al., 1993; Cussler, 1997). Calculated scalar concentration was recorded along transects that spanned the vertical cross-section of the entire fluid domain and were positioned downstream (x) of the mussel siphon (i.e. $x = 0.001, 0.002, 0.003, 0.004, 0.005, 0.01, 0.02, 0.03, 0.04, 0.05, 0.06, 0.07, 0.08, 0.09,$ and 0.1 m downstream). Transects did not interfere with velocity or scalar concentration fields and concentration was recorded every second.

Scalar jets were defined as areas that contained scalar concentrations greater than 20% of the initial concentration at the siphon (Su and Mungal, 2004). The vertical extent of the jet was measured at each downstream transect for each second of the simulation, and the maximum width for each was calculated over 600 or 1300 s. The vertical eddy diffusivity (D) of the fluid in the jet was calculated as

$$D = \frac{W^2 U}{L}, \tag{1}$$

where W is the maximum width of the jet in the vertical direction (m), U is the cross-stream velocity (m s^{-1}), and L is the distance downstream from the siphon (m) (e.g., Okubo and Levin, 2001).

Differences in eddy diffusivity among the different jet behaviors were assessed with ANCOVA, with distance downstream (x) as a covariate. In cases where the assumption of homogenous slopes was violated, pairwise comparisons between behaviors were conducted using the Johnson–Neyman technique, which "allows identification of the range of x values for which there is no significant difference between groups" (White, 2003).

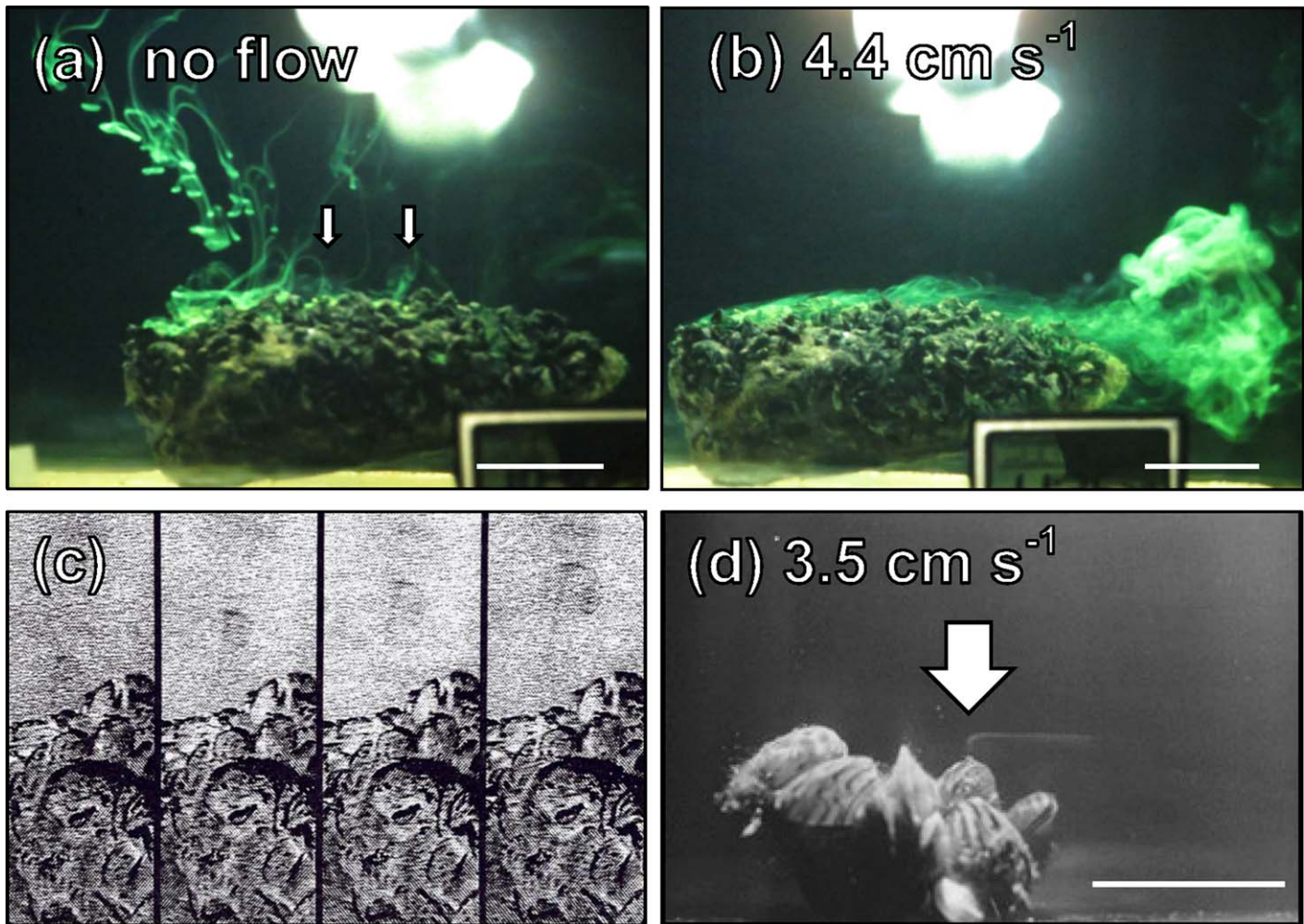To determine the decay rate of scalar concentration associated with jet behavior, maximum concentrations were

Fig. 2. Water motion around dreissenid mussel aggregations. (**a**) Side view of mussel aggregation on a limestone rocks (13.5 × 8 × 5 cm) under no-flow where dye (fluoroscein-labeled algae) was released in a continuous stream in the vertical direction by slowly pulling the injector away from the bottom. Note the retention of dye next to the mussels. Arrows indicate regions where circulation has occurred due to exhalant jets. (**b**) Side view of the same dreissenid mussel aggregation under 4.4 cm s^{-1} with flow from left to right where dye was released at ∼ 2 cm height increments above the mussels. Scale bars for (**a-b**) = 5 cm. (**c**) A time series of a vortex ring generated by exhalant jet from a mussel under no-flow conditions as in (**a**) digitized from video (t = 1, 2.5, 4, and 5 s from left). (**d**) Zebra mussel aggregation at 3.5 cm s^{-1} with exhalant jet extending upward until it is entrained by the bulk flow (indicated by arrow). Scale bar for (**d**) = 2 cm.

normalized by the initial concentration at the siphon (C_{max}/C_0). The distance along the jet scalar centerline (s) was normalized by both the ratio between the jet and cross-stream velocities (r) and the siphon diameter (d). Decay rates were estimated as the slope of the linear regression of C_{max}/C_0 vs. s/rd. For pulsatile jets, C_{max}/C_0 was plotted against x/rd as s could not be reliably estimated for time-dependent behaviors (e.g., estimating the true centerline of the scalar path).

Results

Fluid dynamics of feeding behavior from mussel aggregations

Ambient flow conditions strongly influenced the motion of the algal suspension containing dye around the dreissenid mussel encrusted rock (Fig. 2). Under no-flow, dye released in a continuous vertical stream above the rock remained close to its position of release (Fig. 2a). Dye movements were due to diffusion, which dispersed the dye in all directions, and to potential density differences between the dye and water, which led to drop-like projections in the photograph. At a cross-stream velocity of 4.4 cm s^{-1}, the dye released at ∼2 cm height increments was advected horizontally (Fig. 2b). Dye released on the surface of the rock was retained within the roughness elements of the surface (i.e. the mussels) and was slowed relative to faster-moving dye released 2 cm above the rock (Fig. 2b). Diffusional dispersion and motion just above the surface of the rock were not observed, rather the dye was advected downstream.
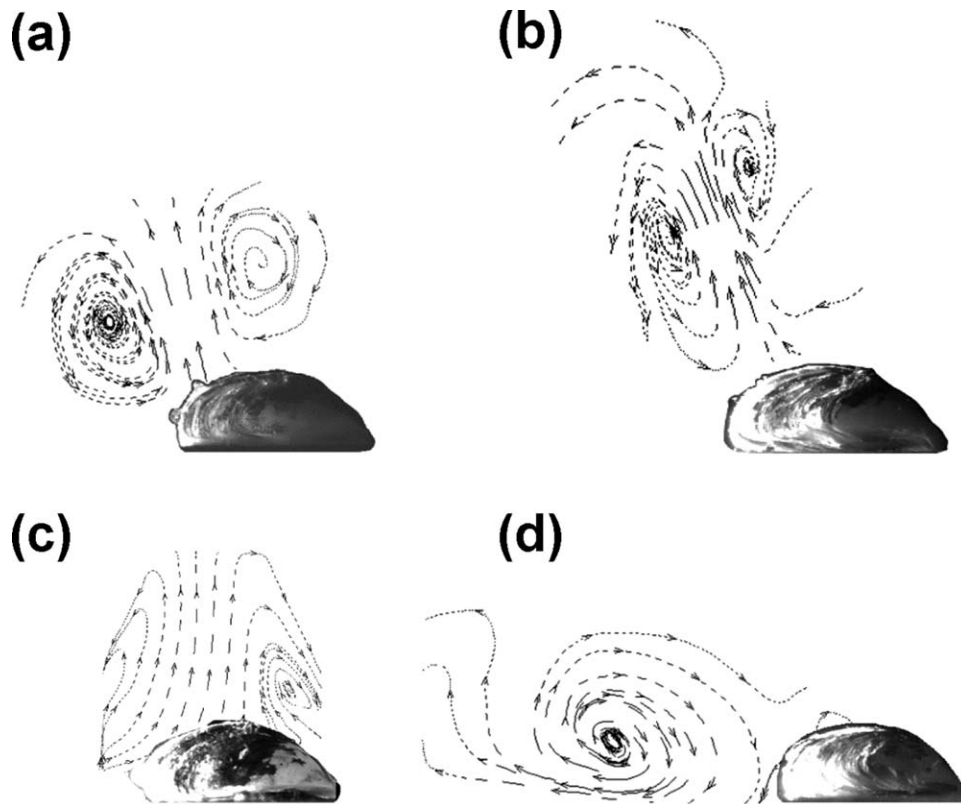
Fig. 3. Streamline plots for exhalant jet behaviors of dreissenid mussels based on particle image velocimetry analysis (PIV) using TecPlot ver. 10 (TecPlot, Bellevue, WA). The arrows indicate the velocity direction, whereas the length of the dashes in the lines indicates the relative magnitude of the velocity. Mussel SL were: (**a**) 2.80 cm (exhalant jet); (**b**) 2.78 cm (streaming); (**c**) 3.18 cm (slow flux) and; (**d**) 3.08 cm (inhalant jet).

Under no flow, dye was released from the exhalant siphons of dreissenid mussels as a result of their suspension-feeding activity (arrows in Fig. 2a). Circulation was revealed to be a free vortex ring that was generated by pulsatile motion of the exhalant siphon, as indicated in a time series ($t = 1$, 2.5, 4, and 5 s from left) of images under no-flow conditions (outer radius of vortex ring was 0.3 and 0.6 cm at $t = 1$ and 4 s, respectively; Fig. 2c). These jets were released intermittently, were not synchronous with each other, and extended to a height of 4–5 cm, above which there was no evidence of their influence on the local fluid. Similar observations were not made at 4.4 cm s^{-1}, presumably because exhalant jets were entrained in the relatively-faster bulk flow above the mussels. Finer-scale flow visualization was required to confirm this assertion.

For small aggregations of zebra mussels, water motion appeared laminar (mean $U = 3.5$ cm s^{-1}). During feeding, mussels opened their valves and extended both inhalant and exhalant siphons into the flow. The exhalant jet from one mussel contained momentum that carried it upward until it was entrained into the bulk flow (indicated by arrow Fig. 2d). In this case, the exhaled jet extended upward ~4 mm before being entrained within the ambient flow of the chamber (1.4 cm above the bottom). This upward motion was sufficient to move the exhaled fluid away from the downstream wake, where it may have been re-entrained by the inhalant siphon.

Characterizing fluid dynamic properties of mussel jets

Four distinct exhalant siphon behaviors were characterized from direct observation and particle image velocimetry, PIV presented as streamline plots (Fig. 3). The first behavior, termed *exhalant jet*, was characterized as a pulsatile jet from the exhalant siphon with mean velocity of 0.22 ± 0.04 (mean $\pm$ SE) cm s^{-1} and mean vorticity of 0.97 ± 0.09 s^{-1} ($n = 16$; Fig. 3a). Zebra mussels displayed a second behavior termed s*treaming jet*, which entailed a continuous jet of moderate velocity and vorticity (0.23 ± 0.03 cm s^{-1} and 0.87 ± 0.11 s^{-1}, respectively; $n = 17$, Fig. 3b). Mussels also displayed a weak, continuous jet from between the valves, termed *slow flux* with much lower velocity and vorticity (0.11 ± 0.02 cm s^{-1} and 0.21 ± 0.04 s^{-1}, respectively; $n = 7$; Fig. 3c). Finally, mussels engaged a "cough-like" response that produced an *inhalant jet* (e.g., exhalant jet from the inhalant siphon) adjacent to the bottom that reached velocities of 0.35 ± 0.07 cm s^{-1} and vorticity of 1.48 ± 0.20 s^{-1} ($n = 10$;
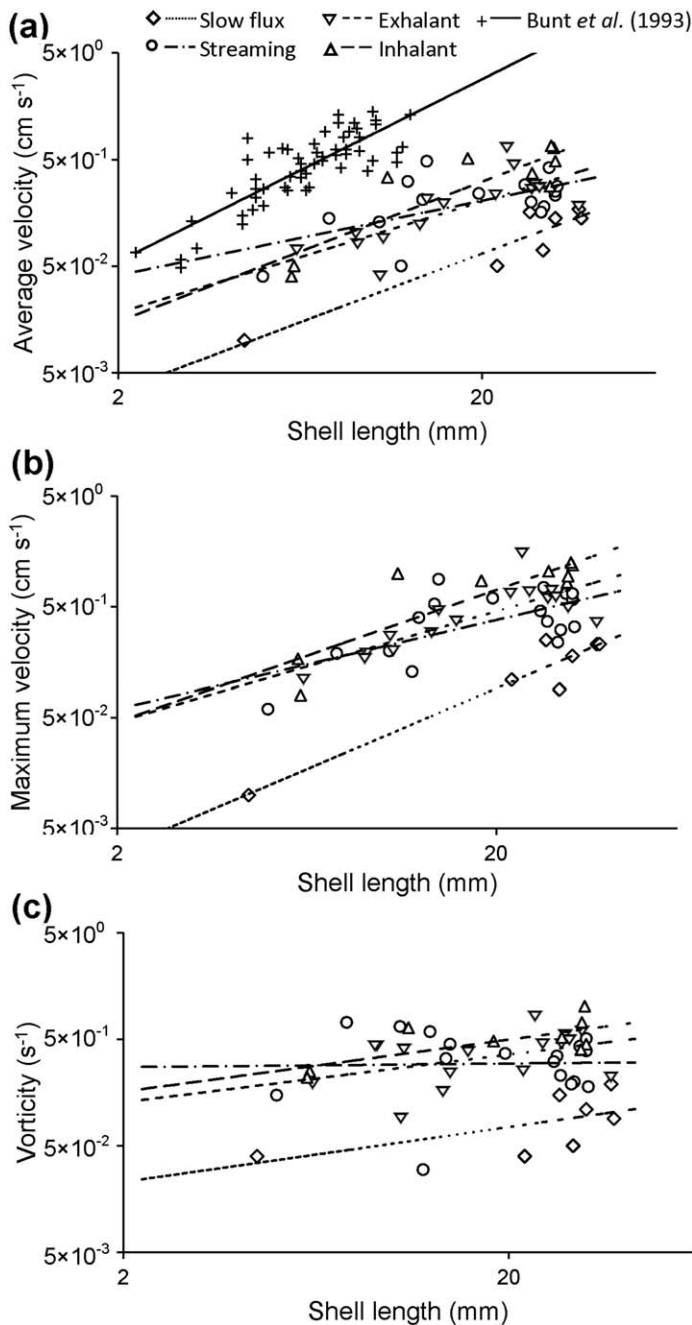
Fig. 4. Hydrodynamic characteristics of exhalant jets: (**a**) mean jet velocities vs. mussel length (including data from Bunt et al., 1993); (**b**) maximum jet velocities; and (**c**) mean jet vorticities. (jet determination and calculations are described in the Methods).

Fig. 3d). Initial algal concentrations for the PIV experiments averaged $3.2 \pm 0.4 \times 10^4$ cells mL^{-1} with no significant differences among trials for the different behaviors ($F_{(3,45)} = 0.890$, $p = 0.478$). Mussels showed no behavioral response to the laser light (e.g., no siphonal retraction/ adjustment) and appeared to feed normally after a short period of acclimation.
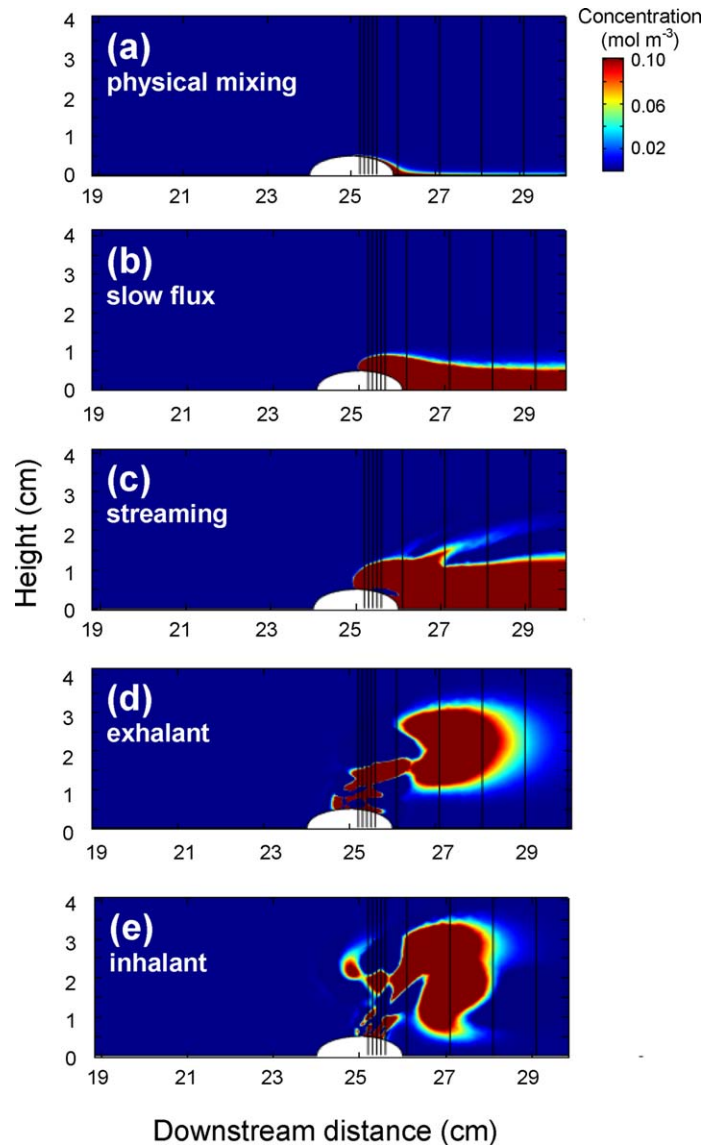
Fig. 5. COMSOL multiphysics modeling of scalar transport from mussel exhalant jets in cross-flow. The simulations were run with: (**a**) physical mixing alone (i.e., no exhalant jet; no-behavior control); (**b**) slow flux; (**c**) streaming; (**d**) exhalant jet at 74 s; and (**e**) inhalant jet at 74 s. Average flow from left to right in the spatial domain (e.g., cross-stream velocity) was 0.1 cm s^{-1}; exhalant behaviors are described in the Methods.

There were significant differences among the four behaviors in term of average velocity ($F_{(3,45)} = 2.973$, $p = 0.029$), where slow flux was significantly slower than streaming, exhalant, and inhalant jets (Bonferroni corrected tests; $p < 0.001$). Similar patterns were found among behaviors for maximum velocity ($F_{(3,45)} = 4.515$, $p = 0.004$), where slow flux was significantly slower than streaming, exhalant and inhalant jets (Bonferroni corrected tests; $p < 0.001$) and streaming was also slower than inhalant jets ($p = 0.032$).
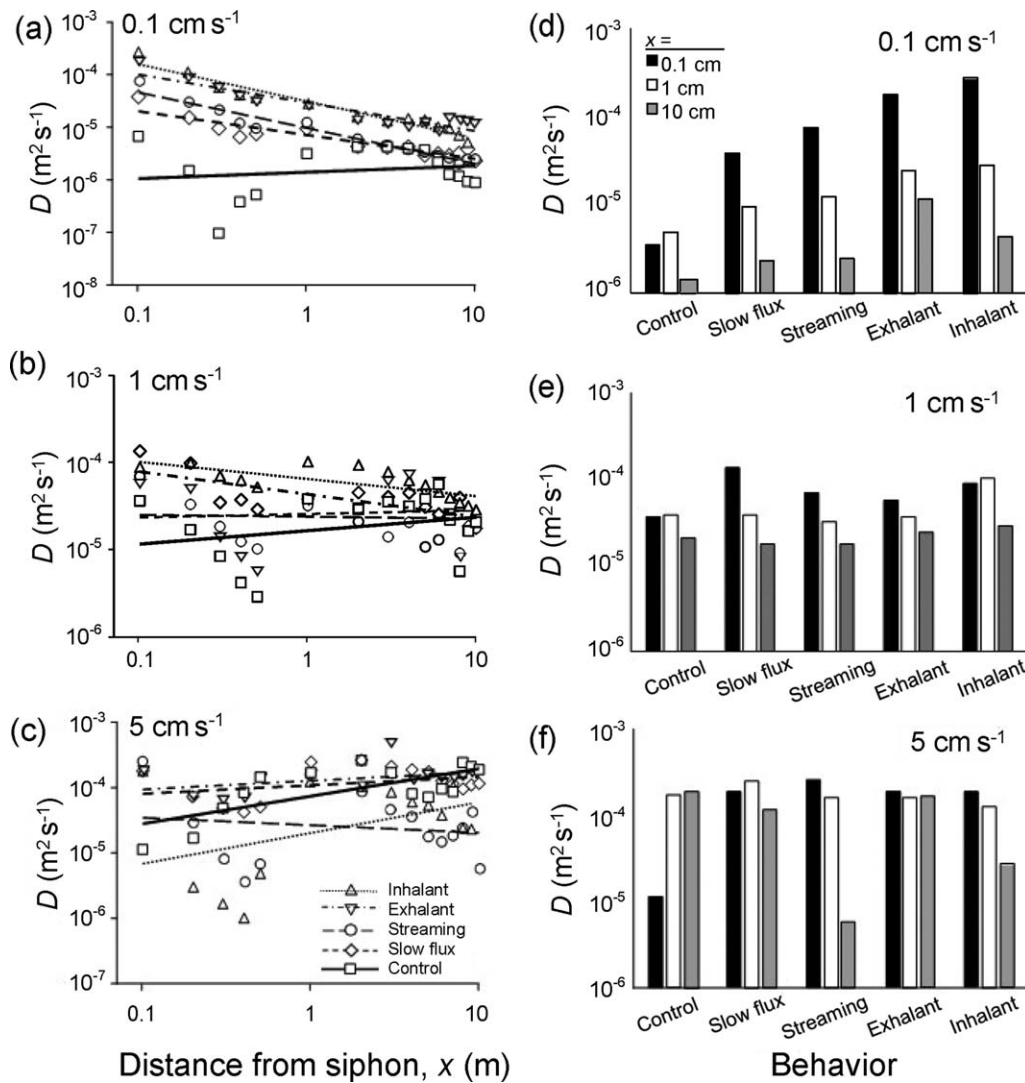
Fig. 6. Modeled effect of exhalant jets on scalar mixing. Vertical eddy diffusivity (D, m^2 s^{-1}) of scalar jet vs. downstream distance (x) at cross-stream velocities of: (**a**) 0.1 cm s^{-1}; (**b**) 1 cm s^{-1}; and (**c**) 5 cm s^{-1} and in a comparison of jet types at $x = 0.1$, 1.0, and 10 cm at cross-stream velocities of: (**d**) 0.1 cm s^{-1}; (**e**) 1 cm s^{-1}; and (**f**) 5 cm s^{-1}. Lines in panels a, b, and c serve to help identify regions of significance in the pairwise comparisons between each treatment and the corresponding controls.

Differences in vorticity were measured among the different behaviors ($F_{(3,45)} = 9.086$, $p < 0.001$), where slow flux displayed significantly lower vorticity than streaming, exhalant, and inhalant jets (Bonferroni corrected tests; $p < 0.001$). There was a significant, positive relationship between average jet velocities and mussel SL (Fig. 4a; $F_{(1,48)} = 10.19$, $p = 0.003$, $R^2 = 0.17$), and maximum jet velocity and shell length (Fig. 4b; $F_{(1,48)} = 7.139$, $p = 0.010$, $R^2 = 0.13$). In contrast, no significant relationship between vorticity and SL was detected (Fig. 4c; $F_{(1,48)} = 0.220$, $p = 0.641$, $R^2 < 0.01$).

The effects of exhalant jets on local mixing

CFD modeling at cross-stream velocity of 0.1 cm s^{-1} revealed that physical mixing in the absence of mussel

behavior generated minimal vertical transport and scalar was largely confined below a height of ~0.8 cm (Fig. 5a). For continuous jets behaviors, the scalar was detected at heights up to ~2 cm, but confined to the region directly adjacent to the bottom (Fig. 5b,c). For pulsatile behaviors, however, the scalar extended to heights of ~4 to 5 cm (Fig. 5d,e), with the majority of the scalar penetrating into the water column above the mussel, and only low concentrations remaining in the region adjacent to the bottom. At faster cross-stream velocities of 1 and 5 cm s^{-1}, the scalar was largely entrained in the cross-flow and limited to heights below ~3 cm regardless of the presence/type of behavior (cf. Fig. 2d).

Jet behavior had pronounced effects on vertical mixing as indicated by the vertical eddy diffusivity, D in the flow
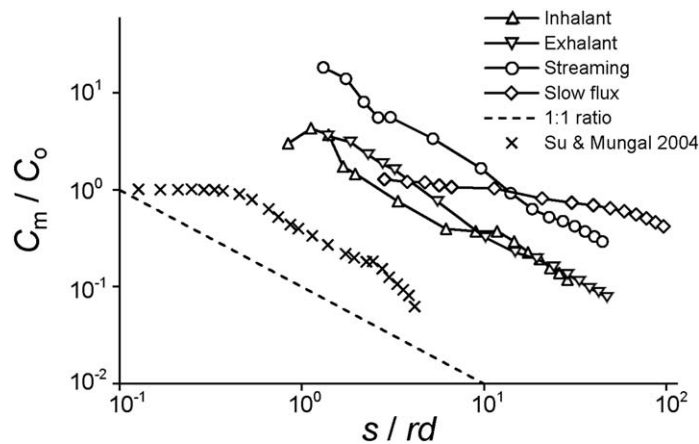
Fig. 7. The decay of maximum scalar concentration (C_m/C_0) in relation to distance along jet centerline (*s*) normalized by the product of the ratio between jet and cross-stream velocities and siphon diameter, *rd*. A comparison with Su and Mungal (2004) is provided.

downstream of the siphon (Fig. 5, 6). At slow flow (e.g., 0.1 cm s^{-1}), *D* was highest for inhalant jets, followed by exhalant, streaming and slow flux, which were all significantly greater than physical mixing alone (i.e. no behavior control; Fig. 6a,d). These differences in *D*, however, diminished at downstream distances (*x*) approaching $\sim 10^{-1}$ m, where for example, the *D* for continuous jets (e.g., streaming and slow flux) was higher than controls in the region of $x < 5 \times 10^{-2}$ m), but were not significantly different farther downstream (Fig. 6a,d; Johnson–Neyman, $p < 0.05$). In contrast, both pulsatile jets (e.g., inhalant and exhalant jets) showed significantly higher *D* compared to physical mixing throughout the entire 10^{-1} m downstream distance (Johnson–Neyman, $p < 0.05$). The results were somewhat similar under a 1 cm s^{-1} cross-stream velocity, where vertical mixing by pulsatile behaviors differed from controls throughout *x* (Johnson–Neyman, $p < 0.05$; Fig. 6b,e), but those of continuous jets were significantly higher than controls for $x < 4 \times 10^{-2}$ m. The results obtained at the fastest cross-stream velocity of 5 cm s^{-1} differed from the above (Fig. 6c,f). Specifically, only the *D* for exhalant jets and slow flux were higher than the control in regions < 2-3×10^{-2} m downstream, respectively (Johnson–Neyman, $p < 0.05$). The *D* of inhalant jets was significantly lower than the no behavior controls throughout *x* and the *D* of streaming jet was lower than the control at downstream distances $> 3 \times 10^{-3}$ m (Johnson–Neyman, $p < 0.05$).

The decay of the maximum scalar concentration along the centerplane of each of the four jets is presented in Fig. 7. Scalar concentration decayed roughly as 1/*s* for exhalant, inhalant and streaming behaviors at slow cross-stream velocity (e.g., the velocity ratio, $r = 2.2$ to 3.5), whereas maximum scalar in the slow flux jet decayed at a slower rate of $s^{-1/3}$.

Discussion

These results demonstrate that dreissenid mussels use a variety of exhalant jet behaviors during their suspension feeding activities. Exhalant jets produced from inhalant and exhalant siphons may be either continuous or pulsatile in nature creating free vortex rings. From a fluid dynamics perspective, exhalant jets generated by the different behaviors spanned a relatively small range of velocities (0.11 to 0.35 cm s^{-1}) and vorticities (0.21 to 1.48 s^{-1}). However, CFD models indicate that these behaviors lead to significant differences in local vertical mixing (Fig. 6), which would aid in the mass transfer of food, dissolved gases and/or waste products as well as biogeochemical processes including nutrient cycling in the near-bed region (Reidenbach et al., 2013; Nalepa and Schloesser, 2014) and hence, could influence ecosystem productivity.

The results of PIV experiment revealed four distinct feeding behaviors, including both continuous and pulsatile jets (Fig. 3). Although continuous jets have been observed in *Dreissena* sp. (Bunt et al., 1993) and in marine mussels (Riisgård et al., 2011), to the best of our knowledge, pulsatile jets have not been documented. Confidence in our observations is based on the use of different sources of mussels, different techniques in different facilities and at different times. Small differences in water temperature between our experiments (17 vs. 19°C) were unlikely to bias our results as dreissenid filtration rates are thermally-invariant at moderate temperatures (e.g., below 28°C; Aldridge et al., 1995). We also documented flow reversals, with strong, pulsatile jets emerging from the inhalant siphon (Fig. 3), likely related to the expulsion of pseudofaeces (Berg et al., 1996). Slow flux from the mantle may be related to the exchange of fluid required for respiration rather than suspension feeding per se. Whereas, this is somewhat speculative, we ensured that this slow-flux result was not an experimental artifact by exposing empty pairs of mussel shells to the laser, which did not lead to any change in the local hydrodynamics.

Jet velocities for all behaviors were positively correlated with mussel SL, consistent with Bunt et al. (1993), who found size dependence of jet velocity in *D. polymorpha* using a different technique, and with reports of higher clearance rates for larger individuals in *D. polymorpha* (Kryger and Riisgård, 1988). It is also consistent with higher pumping rates in marine *Mytilus edulis* that appear to scale with length[2] (i.e. gill area; Jones et al., 1992). Riisgård et al. (2011), however, suggest that jet velocity is independent of SL in *M. edulis* because of varying cross sectional area of their pseudo-siphons created by the "pinching" of mantle tissue. The presence of true siphons in *Dreissena*, while variable in orientation with respect to flow (Ackerman, 1999) and likely static in shape within a given siphonal jet behavior, facilitates the generation of jet vorticity. This occurs via the shear layer in the ambient fluid that undergoes instability in the axial

direction leading to roll up and the formation of coherent axisymmetric vortex rings (Gao and Yu, 2015). The lack of size dependence on jet vorticity may be related to the fact that vorticity, which is generated near the terminus of the siphon (i.e. jet exit), does not vary significantly over this range of SL in terms of cross-sectional shape for a given siphonal behavior to affect the vorticity. Clearly, additional research into the functional morphology of siphonal flows is warranted.

The distribution of scalar for continuous jets was limited to the region adjacent to the bottom boundary (Fig. 5b,c), similar to patterns for continuous jets released from siphons that were flush with the bottom (Monismith et al., 1990). Pulsatile jets distributed scalar into the water column above mussels, away from the bottom (Fig. 5d,e). This was similar to continuous jets that were released from physical models of siphons with increasing height (Monismith et al., 1990). Thus height—whether attained by siphon height or by pulsatile behavior—may help direct scalar away from the local environment surrounding a mussel.

Exhalant jets affected mixing more dramatically at low velocities compared to high velocities (Fig. 6), similar to results from other suspension feeders (O'Riordan et al., 1995; Larsen and Riisgård, 1997; Lassen et al., 2006; van Duren et al., 2006). These data are consistent with observations that well-structured concentration boundary layers form when near-bottom D is low (e.g., 10^{-7} m^2 s^{-1}), but these bottom regions become well mixed when D is elevated (e.g., 10^{-4} m^2 s^{-1}; Larsen and Riisgård, 1997). At low cross-stream velocities, our experiments suggest that near-bottom D ranged from 10^{-6} m^2 s^{-1} for physical mixing alone to 10^{-4} m^2 s^{-1} for inhalant jets. This supports the idea that mussel behavior is an important factor in determining patterns of near-bottom mixing, including ecologically-relevant scalars (e.g., gases, nutrients). Whether or not mussels switch behavior to enhance mixing according to the ambient conditions is not known and is a subject that warrants further investigation.

Under low flow, pulsatile jets displayed higher D compared with continuous jets (Fig. 6), presumably due to the vortex ring formed in pulsed jets. This is consistent with results showing higher volumetric entrainment in pulsatile vs. continuous jets (Kouros et al., 1993). Mixing is enhanced by the vortex ring (e.g., Fig. 5d,e) for both exhalant and inhalant jets ($r = 2.2$ and 3.5, respectively), consistent with vortex ring formation when $r > 2$ (Sau and Mahesh, 2008). Such differences, however, may be minimized at faster cross-stream velocities as the vortex structure dissipates. Under these conditions, mixing is largely due to the horseshoe vortex that forms around the jet as it enters the cross-flow (Crow and Champagne, 1971; Eckman and Nowell, 1984). Indeed, vortex shedding from jets in cross-flow can affect scalar distribution for several centimeters downstream (Ertman and Jumars, 1988).

Maximum scalar concentration decayed roughly as s^{-1} for inhalant, exhalant, and streaming jets at a cross-flow velocity of 0.1 cm s^{-1}. Reynolds numbers (Re) based on jet velocity and jet diameter (Re_{jet}) ranged from 4.4 to 6.8 and the ratio of jet velocity to cross-stream velocity (r) ranged from 2 to 4. This s^{-1} decay is consistent with previous reports of jet behavior in cross-stream, where $r = 5$ to 25 and $Re_{\text{jet}} = 8,400$ to 41,500 (Smith and Mungal, 1998; Su and Mungal, 2004). Only in the slow flux, where $r = 1$ and $Re_{\text{jet}} = 2.2$, did scalar decay differ dramatically from the power law scaling described for pure jet behavior (e.g., $s^{-1/3}$ vs. $s^{-2/3}$) (Fig. 7). Moreover, reduced decay for the slow flux reinforces the notion that these jets had limited mixing compared to the other behaviors (e.g., lower D; Fig. 6).

Model results indicate that continuous exhalant jets extend ~1 to 2 cm above the siphon under slow flow, which is in agreement with direct observations of dreissenid mussels (Figs. 2, 5; Bunt et al., 1993). However, pulsatile jets reached greater heights through the free vortex rings compared to continuous jets (Fig. 5). This is consistent with results that artificially pulsed jets penetrate significantly farther into the crossflow than steady jets (Eroglu and Breidenthal, 2001). It is intriguing to suggest that increased mixing due to exhalant jets may support higher productivity at low flows, when suspension feeders may become mass-transfer limited (Frechette et al., 1989; Wildish and Kristmanson, 1997; Ackerman, 1999; Saurel et al., 2013). It is relevant to note that bottom topography, oscillatory flows, and interactions among exhalant jets may also influence mixing (O'Riordan et al., 1993; Folkard and Gascoigne, 2009). Regardless, these results demonstrate that dreissenid mussels use a diverse set of exhalant behaviors, which lead to different levels of local mixing that may support higher productivity and may help to explain their large impacts on aquatic ecosystems (Schloesser et al., 1996; Bódis et al., 2014).

References

Ackerman, J. D. 1999. Effect of velocity on the filter feeding of dreissenid mussels (*Dreissena polymorpha* and *Dreissena bugensis*): Implications for trophic dynamics. Can. J. Fish. Aquat. Sci. **56**: 1551–1561. doi:10.1139/cjfas-56-9-1551

Ackerman, J. D. 2014. Role of fluid dynamics in dreissenid mussel biology, p. 471–483 *In* T. F. Nalepa and D. W. Schloesser [eds.], Quagga and zebra mussels: Biology, impact, and control, 2nd ed. CRC Press. doi:10.1201/b15437-36

Ackerman, J. D., M. R. Loewen, and P. F. Hamblin. 2001. Benthic-pelagic coupling over a zebra mussel reef in western Lake Erie. Limnol. Oceanogr. **46**: 892–904. doi:10.4319/lo.2001.46.4.0892

Ackerman, J. D., and M. T. Nishizaki. 2004. The effect of velocity on the suspension feeding and growth of the marine mussels *Mytilus trossulus* and *M. californianus*:

Implications for niche separation. J. Mar. Syst. **49**: 195–207. doi:10.1016/j.jmarsys.2003.06.004

Aldridge, D. W., B. S. Payne, and A. C. Miller. 1995. Oxygen consumption, nitrogenous excretion, and filtration rates of *Dreissena polymorpha* at acclimation temperatures between 20 and 32 C. Can. J. Fish. Aquat. Sci. **52**: 1761–1767. doi:10.1139/f95-768

Berg, D. J., S. W. Fisher, and P. F. Landrum. 1996. Clearance and processing of algal particles by zebra mussels (*Dreissena polymorpha*). J. Great Lakes Res. **22**: 779–788. doi:10.1016/S0380-1330(96)70996-6

Boegman, L., M. R. Loewen, P. F. Hamblin, and D. A. Culver. 2008. Vertical mixing and weak stratification over zebra mussel colonies in western Lake Erie. Limnol. Oceanogr. **53**: 1093–1110. doi:10.4319/lo.2008.53.3.1093

Bódis, E., B. Tóth, and R. Sousa. 2014. Impact of *Dreissena* fouling on the physiological condition of native and invasive bivalves: Interspecific and temporal variations. Biol. Invasions **16**: 1373–1386. [CrossRef][10.1007/s10530-013-0575-z][Mismatch]doi:10.1007/s10530-013-0575-z doi:10.1007/s10530-013-0575-z

Bunt, C. M., H. J. Maclsaac, and W. G. Sprules. 1993. Pumping rates and projected filtering impacts of juvenile zebra mussels (*Dreissena polymorpha*) in western Lake Erie. Can. J. Fish. Aquat. Sci. **50**: 1017–1022. doi:10.1139/f93-117

Canfield, D. E., and W. J. Green. 1985. The cycling of nutrients in a closed-basin Antarctic lake: Lake Vanda. Biogeochemistry. **1**: 233–256. doi:10.1007/BF02187201

Cha, Y., C. A. Stow, and E. S. Bernhardt. 2013. Impacts of dreissenid mussel invasions on chlorophyll and total phosphorus in 25 lakes in the USA. Freshw. Ecol. **58**: 192–296. doi:10.1111/fwb.12050

Conroy, J. D., D. D. Kane, D. M. Dolan, W. J. Edwards, M. N. Charlton, and D. A. Culver. 2005. Temporal trends in Lake Erie plankton biomass: Roles of external phosphorus loading and dreissenid mussels. J. Great Lakes Res. **31**: 89–110. doi:10.1016/S0380-1330(05)70307-5

Crow, S. C., and F. H. Champagne. 1971. Orderly structure in jet turbulence. J. Fluid Mech. **48**: 547–591. doi:10.1017/S0022112071001745

Cussler, E. L. 1997. Diffusion: Mass transfer in fluid systems. Cambridge Univ. Press.

Davidson, P. A. 2004. Turbulence: An introduction for scientists and engineers. Oxford Univ. Press.

Eckman, J. E., and A. R. M. Nowell. 1984. Boundary skin friction and sediment transport about an animal-tube mimic. Sedimentology **31**: 851–862. doi:10.1111/j.1365-3091.1984.tb00891.x

Eroglu, A., and R. E. Breidenthal. 2001. Structure, penetration, and mixing of pulsed jets in crossflow. AIAA J. **39**: 417–423. doi:10.2514/2.1351

Ertman, S. C., and P. A. Jumars. 1988. Effects of bivalve siphonal currents on the settlement of inert particles and larvae. J. Mar. Res. **46**: 797–813. doi:10.1357/002224088785113342

Folkard, A. M., and J. C. Gascoigne. 2009. Hydrodynamics of discontinuous mussel beds: Laboratory flume simulations. J. Sea Res. **62**: 250–257. doi:10.1016/j.seares.2009.06.001

Frechette, M., C. A. Butman, and W. R. Geyer. 1989. The importance of boundary-layer flows in supplying phytoplankton to the benthic suspension feeder, *Mytilus edulis* L. Limnol. Oceanogr. **34**: 19–36. doi:10.4319/lo.1989.34.1.0019

Gao, L., and S. C. Yu. 2015. Starting jets and vortex ring pinch-off, p. 1–31. *In* D. T. New and S. C. Yu [eds.], Vortex rings and jets. Springer.

Gilli, J. P., and R. Coma. 1998. Benthic suspension feeders: Their paramount role in littoral marine food webs. Trends Ecol. Evol. **13**: 316–321. doi:10.1016/S0169-5347(98)01365-2

Greene, S., Y. R. McElarney, and D. Taylor. 2015. Water quality effects following establishment of the invasive *Dreissena polymorpha* (Pallas) in a shallow eutrophic lake: Implications for pollution mitigation measures. Hydrobiologia **743**: 237–253. doi:10.1007/s10750-014-2041-z

Hecky, R. E., R. E. Smith, D. R. Barton, S. J. Guildford, W. D. Taylor, M. N. Charlton, and T. Howell. 2004. The nearshore phosphorus shunt: A consequence of ecosystem engineering by dreissenids in the Laurentian Great Lakes. Can. J. Fish. Aquat. Sci. **61**: 1285–1293. doi:10.1139/f04-065

Higgins, S. N., B. Althouse, S. P. Devlin, Y. Vadeboncoeur, and M. J. Vander Zanden. 2014. Potential for large-bodied zooplankton and dreissenids to alter the productivity and autotrophic structure of lakes. Ecology **95**: 2257–2267. doi:10.1890/13-2333.1

Jones, H. D., O. G. Richards, and T. A. Southern. 1992. Gill dimensions, water pumping rate and body size in the mussel *Mytilus edulis* L. J. Exp. Mar. Biol. Ecol. **155**: 213–237. doi:10.1016/0022-0981(92)90064-H

Jørgensen, C. B. 1990. Bivalve filter feeding: Hydrodynamics, bioenergetics, physiology and ecology. Olsen & Olsen.

Kouros, H., R. Medina, and H. Johari. 1993. Spreading rate of an unsteady turbulent jet. AIAA J. **31**: 1524–1526. doi:10.2514/3.49085

Kryger, J., and H. U. Riisgård. 1988. Filtration rate capacities in 6 species of European freshwater bivalves. Oecologia **77**: 34–38. doi:10.1007/BF00380921

Larsen, P. S., and H. U. Riisgård. 1997. Biomixing generated by benthic filter feeders: A diffusion model for near-bottom phytoplankton depletion. J. Sea Res. **37**: 81–90. doi:10.1016/S1385-1101(97)00009-9

Lassen, J., M. Kortegard, H. U. Riisgård, M. Friedrichs, G. Graf, and P. S. Larsen. 2006. Down-mixing of phytoplankton above filter-feeding mussels - interplay between water

flow and biomixing. Mar. Ecol. Prog. Ser. **314**: 77–88. doi: 10.3354/meps314077

Monismith, S., J. Koseff, J. Thompson, C. O'Riordan, and H. Nepf. 1990. A study of model bivalve siphonal currents. Limnol. Oceanogr. **35**: 680–696. doi:10.4319/lo.1990.35.3.0680

Nalepa, T. F., and D. Schloesser. 2014. Quagga and zebra mussels: Biology, impacts, and control, 2nd ed. CRC Press.

Nishizaki, M. T., and J. D. Ackerman. 2005. A secondary chemical cue facilitates juvenile-adult postsettlement associations in red sea urchins. Limnol. Oceanogr. **50**: 354–362. doi:10.4319/lo.2005.50.1.0354

Nishizaki, M. T., and E. Carrington. 2014. Behavioral responses to water flow and temperature influence feeding in the barnacle, *Balanus glandula*. Mar. Ecol. Prog. Ser. **507**: 207–218. doi:10.3354/meps10848

North, R. L., R. E. Smith, R. E. Hecky, D. C. Depew, L. F. León, M. N. Charlton, and S. J. Guildford. 2012. Distribution of seston and nutrient concentrations in the eastern basin of Lake Erie pre-and post-dreissenid mussel invasion. J. Great Lakes Res. **38**: 463–476. doi:10.1016/j.jglr.2012.06.012

Okubo, A., and S. A. Levin. 2001. Diffusion and ecological problems: Modern perspectives. Springer.

O'Riordan, C. A., S. G. Monismith, and J. R. Koseff. 1993. A study of concentration boundary-layer formation over a bed of model bivalves. Limnol. Oceanogr. **38**: 1712–1729. doi:10.4319/lo.1993.38.8.1712

O'Riordan, C., S. Monismith, and J. Koseff. 1995. The effect of bivalve excurrent jet dynamics on mass transfer in a benthic boundary layer. Limnol. Oceanogr. **40**: 330–344. doi:10.4319/lo.1995.40.2.0330

Reidenbach, M. A., P. Berg, A. Hume, J. C. R. Hansen, and E. R. Whitman. 2013. Hydrodynamics of intertidal oyster reefs: The influence of boundary layer flow processes on sediment and oxygen exchange. Limnol. Oceanogr. Fluids Environ. **3**: 225–239. doi:10.1215/21573689-2395266

Riisgård, H. U., and P. S. Larsen. 2010. Particle capture mechanisms in suspension-feeding invertebrates. Mar. Ecol. Prog. Ser. **418**: 255–293. doi:10.3354/meps08755

Riisgård, H. U., B. H. Jørgensen, K. Lundgreen, F. Storti, J. H. Walther, K. E. Meyer, and P. S. Larsen. 2011. The exhalant jet of mussels *Mytilus edulis*. Mar. Ecol. Prog. Ser. **437**: 147–164. doi:10.3354/meps09268

Saltzman, E. S., D. B. King, K. Holmen, and C. Leck. 1993. Experimental determination of the diffusion coefficient of dimethylsulfide in water. J. Geophys. Res. Oceans **98**: 16481–16486. doi:10.1029/93JC01858

Saurel, C., J. K. Petersen, P. J. Wiles, and M. J. Kaiser. 2013. Turbulent mixing limits mussel feeding: Direct estimates of feeding rate and vertical diffusivity. Mar. Ecol. Prog. Ser. **485**: 105–121. doi:10.3354/meps10309

Sau, R., and K. Mahesh. 2008. Dynamics and mixing of vortex rings in crossflow. J. Fluid Mech. **604**: 389–409. doi:10.1017/S0022112008001328

Schloesser, D. W., and W. P. Kovalak. 1991. Infestation of unionids by *Dreissena polymorpha* in a power plant canal in Lake Erie. United States Geological Survey.

Schloesser, D. W., T. F. Nalepa, and G. L. Mackie. 1996. Zebra mussel infestation of unionid bivalves (Unionidae) in North America. Am. Zool. **36**: 300–310. doi:10.1093/icb/36.3.300

Schneider, D. W., S. P. Madon, J. A. Stoeckel, and R. E. Sparks. 1998. Seston quality controls zebra mussel (*Dreissena polymorpha*) energetics in turbid rivers. Oecologia **117**: 331–341. doi:10.1007/s004420050666

Sebens, K., G. Sarà, and M. T. Nishizaki. In press. Energetics, particle capture and growth dynamics of benthic suspension feeders. *In* S. Ross, L. Bramanti, A. Gori, and C. Orejas Saco del Valle [eds.], Marine animal forests: The ecology of benthic biodiversity hotspots. Springer.

Smaal, A. C., J. H. G. Verbagen, J. Coosen, and H. A. Haas. 1986. Interaction between seston quantity and quality and benthic suspension feeders in the Oosterschelde, the Netherlands. Ophelia **26**: 385–399. doi:10.1080/00785326.1986.10422002

Smith, S. H., and M. G. Mungal. 1998. Mixing, structure and scaling of the jet in crossflow. J. Fluid Mech. **357**: 83–122. doi:10.1017/S0022112097007891

Smith, R. E., C. C. Parrish, D. C. Depew, and A. Ghadouani. 2007. Spatial patterns of seston concentration and biochemical composition between nearshore and offshore waters of a Great Lake. Freshw. Biol. **52**: 2196–2210. doi:10.1111/j.1365-2427.2007.01848.x

Stoeckmann, A. M., and D. W. Garton. 1997. A seasonal energy budget for zebra mussels (*Dreissena polymorpha*) in western Lake Erie. Can. J. Fish. Aquat. Sci. **54**: 2743–2751. doi:10.1139/cjfas-54-12-2743

Su, L. K., and M. G. Mungal. 2004. Simultaneous measurements of scalar and velocity field evolution in turbulent crossflowing jets. J. Fluid Mech. **513**: 1–45. doi:10.1017/S0022112004009401

Tyner, E. H., H. A. Bootsma, and B. M. Lafrancois. 2015. Dreissenid metabolism and ecosystem-scale effects as revealed by oxygen consumption. J. Great Lakes Res. **41**: 27–37. doi:10.1016/j.jglr.2015.05.009

Vanderploeg, H. A., J. R. Liebig, T. F. Nalepa, G. L. Fahnenstiel, and S. A. Pothoven. 2010. *Dreissena* and the disappearance of the spring phytoplankton bloom in Lake Michigan. J. Great Lakes Res. **36**: 50–59. doi:10.1016/j.jglr.2010.04.005

van Duren, L. A., P. M. J. Herman, A. J. J. Sandee, and C. H. R. Heip. 2006. Effects of mussel filtering activity on boundary layer structure. J. Sea Res. **55**: 3–14. doi:10.1016/j.seares.2005.08.001

White, C. R. 2003. Allometric analysis beyond heterogeneous regression slopes: Use of the Johnson-Neyman Technique in comparative biology. Physiol. Biochem. Zool. **76**: 135–140. doi:10.1086/367939

Wildish, D. J., and D. D. Kristmanson. 1997. Benthic suspension feeders and flow. Cambridge Univ. Press.

Acknowledgments

Conflict of Interest

None declared.